Eavesdropper Localization in Random Walk Channels

Weisi Guo[1], Yansha Deng[2], Bin Li[3], Chenglin Zhao[3], Arumugam Nallanathan[2]

***Abstract*—Eavesdroppers are notoriously difficult to detect and locate in traditional wireless communication systems, especially if they are silent. We show that in molecular communications, where information molecules undergo random walk propagation, eavesdropper detection and localization is possible if the eavesdropper is an absorbing receiver. This is due to the fact that the random walk process has a finite return probability and the eavesdropper is a detectable energy sink of which its location can be reverse estimated.**

***Index Terms*—molecular communication, security.**

I. Introduction

Molecular communications has gained significant research attention in recent years, providing an alternative and attractive way to communicate at small-scales and in biological environments [1], [2]. Its applications include targeted drug delivery [1], [3], [4] and industrial monitoring [2]. In order for small devices to communicate in a secure manner [5], detection of eavesdroppers is important [6]. Yet, this area has received little attention and we believe this paper is the first to examine how to detect molecular communication eavesdroppers.

In traditional radio-frequency (RF) systems, silent eavesdroppers are notoriously difficult to detect and localize. Whilst unintentional circuit leakage radiation emitted by all RF systems can aid detection [7], this is not possible for molecular systems. In molecular communications, the data bearing molecules undergo diffusion (see Fig. 1), and one unique feature of the random walk (RW) channel is that the molecules have a finite probability to travel in an opposite direction without reflection. This property can be exploited to detect the silent eavesdropper.

In this paper, our contribution is that we exploit the aforementioned attributes of the RW channel to show that an eavesdropper can be detected and its position accurately estimated. We do so for an eavesdropper that is positioned at an arbitrary location and validate our closed-form expressions through molecule dynamic simulations. As far as we are aware, no existing molecular communications work has considered how to detect the presence of another receiver and locate it in a RW channel.

II. Formulation

The Brownian motion of information molecules can generally be described by the RW model (see Fig. 1). In normal diffusion, the probability density function (PDF) of the molecule position at displacement x from the transmitter and at any given time t is [8]

$$P(x,t) = \frac{1}{(4\pi Dt)^{1/2}} \exp\left(-\frac{x^2}{4Dt}\right), \tag{1}$$

where D is the diffusion coefficient (mass diffusivity). Throughout this paper, we consider the hitting distribution of one-dimensional (1-D) molecular motion with no more than two receivers, and generalization to higher dimensions with multiple receivers is left for future work. The 1-D equations are appropriate for modeling semi-infinite channels (i.e., pipes), where the length dimension is significantly larger than the width and height. As shown in Fig. 1, a transmitter lies at $x = 0$ and emits information molecules that can be absorbed by fully absorbing receivers (modelled as boundary walls). We first present the molecule position PDF for symmetrical boundaries and then derive it for asymmetric boundaries.

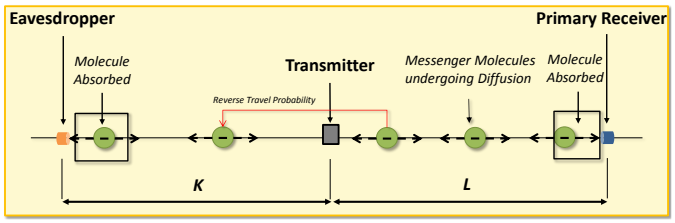

Fig. 1. Illustration of eavesdropping in 1-D molecular communication channel.

A. Single Boundary

In the presence of a single boundary wall (primary receiver) at $x = +L$, the typical scenarios include: i) reflection (receiver rejects molecules, with PDF $\hat{P}$), and ii) absorption (receiver absorbs molecules, with PDF $\check{P}$) at the boundary wall. By exploiting the linear property of the RW process, the PDF of the free molecule can be expressed as a superposition of the original boundary-free RW process $P(x,t)$ and another RW process starting at a negative mirror location $P(x-2L,t)$ (see Fig. 2**a**), such that the PDF of the *free molecules* is [9]

$$\begin{aligned} \hat{P}_1(x,L,t) &= P(x,t) + P(x-2L,t) \quad \text{reflect}, \\ \check{P}_1(x,L,t) &= P(x,t) - P(x-2L,t) \quad \text{absorb}. \end{aligned} \tag{2}$$

These equations satisfy the boundary conditions of having no flux at the boundary (absorbing or reflecting wall), and also no concentration at the boundary for an absorbing wall. If one is interested in the number of molecules absorbed by the receiver at position $+L$, it can be shown that the total number

[1]W. Guo is with the University of Warwick, UK. [2]Y. Deng and A. Nallanathan are with King's College London, UK. [3]B. Li and C. Zhao is with Beijing University of Posts and Telecommunications, China. This work is funded by Royal Society and NSFC Grant IE150708.

the absorbed molecules up to time t is

$$H_1(L,t) = 1 - \int_{x=-\infty}^{+L} \check{P}_1(x,L,t)\,\mathrm{d}x = \mathrm{erfc}\left(\frac{L}{\sqrt{4Dt}}\right), \quad (3)$$

and the rate of molecule absorption is given by: $h_1(L,t) = \mathrm{d}H_1(L,t)/\,\mathrm{d}t = \frac{L}{\sqrt{4\pi Dt^3}}\exp(-L^2/4Dt)$, which is well established, and can be proven using simple initial and boundary conditions [10], but not easily expandable to multiple absorbing receivers.

B. Symmetrical Boundaries

In the presence of two symmetrically placed boundary walls at $x = -L$ and $x = +L$, we analyse the PDF for reflection and absorption. The solutions are also well known and some of which can be found in [9]. As before, the PDF of the free molecule can be expressed as a superposition of the original boundary-free RW process $P(x,t)$ and mirrored RW processes. As shown in Fig. 2**b**, the complication arises when the initial negative mirrors from $x = \pm 2L$ (for the $x = \pm L$ walls) will cause a reminder *residue* term at the opposite $x = \mp L$ walls. The residue term at each wall is $-P(3L,t)$. Hence, there is a need to create multiple positive mirrors that act to cancel each other out at $x = \pm 4L$. Using geometric reasoning, the negative images are at $\pm 2L$ and the positive images at $\pm 4L$. Hence, the free molecules' PDF for symmetric absorbing walls is

$$\check{P}_{2s}(x,L,t) = \sum_{n=-\infty}^{+\infty}\Big[P(x+4nL,t) - P(x+(4n-2)L,t)\Big]. \quad (4)$$

Similarly, it can be shown that the free molecules' PDF for symmetric reflecting walls is: $\hat{P}_{2s}(x,L,t) = \sum_{n=-\infty}^{+\infty} P(x+2nL,t)$. The PDF for multiple boundaries can be approximated by only considering the first few mirror terms (i.e., for small values of n (e.g., n= -1, 0, 1)), if the absorbers are sufficiently far away from the transmitter.

C. Asymmetrical Absorbing Boundaries

Most existing applied physics and statistics research has focused on singular or symmetrical boundaries [9], and asymmetric boundaries are more complex and received less attention in literature. In this paper, we consider the general case of two absorbing walls placed at x=-K and x=+L, where K≠ L and the parameters can take on any values. The geometric reasoning (similar to the symmetric case [9]) is based on cancelling out the molecule residue at the walls, so that the boundary conditions of zero flux and zero concentration are maintained. This is achieved with the aid of negative and positive mirror pulses, which are transmitted from a cascade of mirrors, which extend in distance from 0 to +∞ on the positive axis (wall L side) and from 0 to -∞ on the negative axis (wall K side). In effect, the complex diffusion equation is approximated by an infinite series of hitting distributions, and the mirrors form an intuitive analogy (see Fig.2c).

- the positive images (including original signal) are at $x - 2n(L+K)$: $P^{+}_{-\infty,+\infty} = \sum_{n=-\infty}^{+\infty} P(x-2n[L+K],t)$;

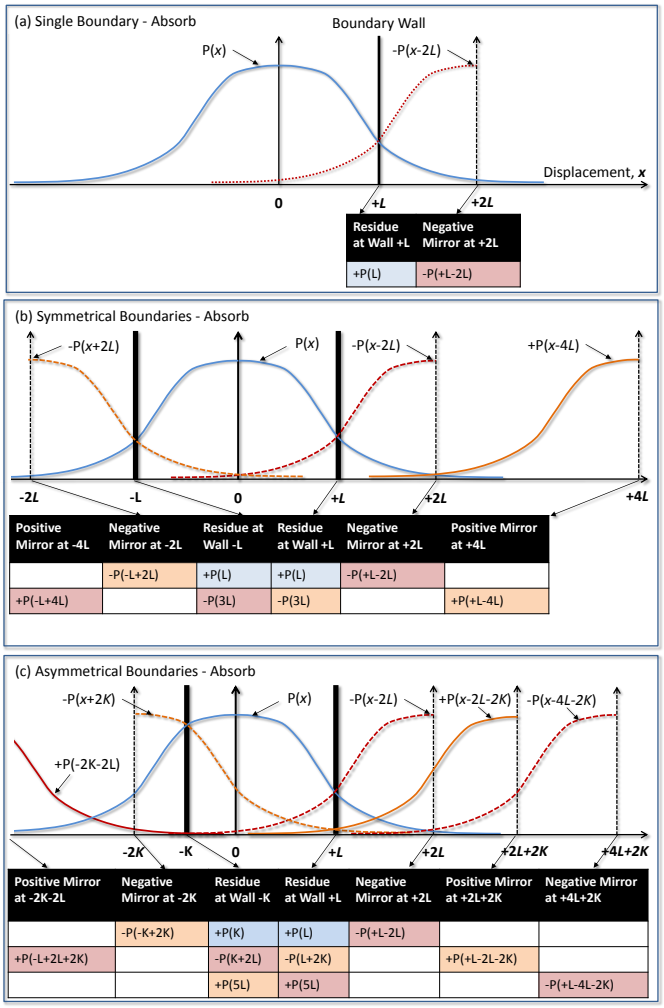

Fig. 2. Illustration of diffusion with mirrored processes and boundary residue cancellation for a) a single absorbing boundary, b) 2 symmetrical absorbing boundaries, and c) 2 asymmetrical absorbing boundaries.

- the negative images in the positive axis are at $x+2[nL+(n-1)K]$: $P^{-}_{-\infty,-1} = -\sum_{n=+1}^{+\infty} P(x-2[nL+(n-1)K],t)$;
- the negative images in the negative axis are at $x+2[nK+(n-1)L]$: $P^{-}_{+1,+\infty} = -\sum_{n=-1}^{-\infty} P(x-2[nK+(n+1)L],t)$;

The resulting free molecules' PDF for asymmetric absorbing walls is

$$\begin{aligned}\check{P}_{2a}(x,L,K,t) &= P^{+}_{-\infty,+\infty} + P^{-}_{-\infty,-1} + P^{-}_{+1,+\infty} \\ &= \sum_{n=-\infty}^{+\infty} P(x-x_a,t) - \sum_{n=+1}^{+\infty} P(x-x_b,t) \\ &\quad - \sum_{n=-1}^{-\infty} P(x-x_c,t),\end{aligned} \quad (5)$$

with $x_a = 2n(L+K)$, $x_b = 2\left[nL+(n-1)K\right]$, and $x_c = 2\left[nK+(n+1)L\right]$. It can be observed that Eq. (5) is reduced to the symmetric case given by Eq. (4) when $K = L$.

Using similar logic from Eq. (3), the fraction of molecules

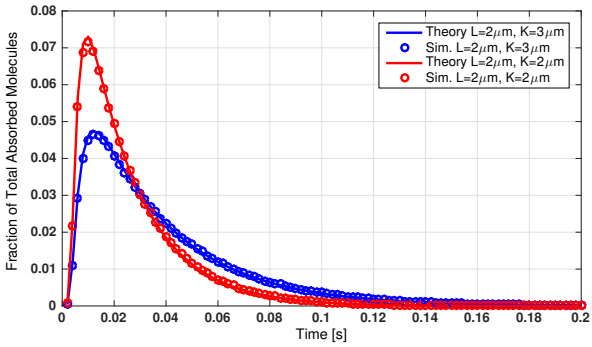

Fig. 3. The fraction of newly absorbed molecules at both receivers. Simulation parameters: D = 79.4μm^2/s, $L = 2\mu$m, $K = 3\mu$m, T_s = 2ms, simulation step $\delta_t = 10^{-5}$s, and repetition is 1000.

absorbed by both receivers is derived as

$$\begin{aligned} H_{2a}(x,L,K,t) &= 1 - \int_{-K}^{+L} \check{P}_{2a}(x,L,K,t)\,\mathrm{d}x \\ &= 1 - \sum_{n=-\infty}^{\infty} \frac{1}{2}\left(\mathrm{erf}\left(\frac{L-x_a}{\sqrt{4Dt}}\right) - \mathrm{erf}\left(\frac{-K-x_a}{\sqrt{4Dt}}\right)\right) \\ &\quad + \sum_{n=1}^{\infty} \frac{1}{2}\left(\mathrm{erf}\left(\frac{L-x_b}{\sqrt{4Dt}}\right) - \mathrm{erf}\left(\frac{-K-x_b}{\sqrt{4Dt}}\right)\right) \\ &\quad + \sum_{n=-\infty}^{-1} \frac{1}{2}\left(\mathrm{erf}\left(\frac{L-x_c}{\sqrt{4Dt}}\right) - \mathrm{erf}\left(\frac{-K-x_c}{\sqrt{4Dt}}\right)\right). \end{aligned} \tag{6}$$

The expected fraction of newly absorbed molecules (both receivers) during any sampling time T_s can be derived as

$$\begin{aligned} h^*_{2a}(x,L,K,t,t+T_s) = \\ H_{2a}(x,L,K,t+T_s) - H_{2a}(x,L,K,t), \end{aligned} \tag{7}$$

where for the extremely small T_s, we derive the resulting rate of absorption as

$$\begin{aligned} h_{2a}(x,L,K,t) &= \frac{\mathrm{d}H_{2a}(L,K,t)}{\mathrm{d}t} \\ &= \frac{1}{\sqrt{4Dt^3}}\Bigg[\sum_{n=-\infty}^{+\infty}(x-x_a)\exp\left(\frac{x-x_a}{\sqrt{4Dt}}\right)\Bigg|_{-K}^{+L} \\ &\quad - \sum_{n=+1}^{+\infty}(x-x_b)\exp\left(\frac{x-x_b}{\sqrt{4Dt}}\right)\Bigg|_{-K}^{+L} \\ &\quad - \sum_{n=-1}^{-\infty}(x-x_c)\exp\left(\frac{x-x_c}{\sqrt{4Dt}}\right)\Bigg|_{-K}^{+L}\Bigg]. \end{aligned} \tag{8}$$

In Fig. 3, we validate our derived results for the expected fraction of newly absorbed molecules (both receivers) during any sampling time T_s in Eq. (7) via the molecule-based simulation for both symmetrical and asymmetrical receivers. The details of particle-based simulation follows from [11].

III. Detection and Localization

Having formulated the probability functions for RW in the presence of reflecting and absorbing receivers, this section will devise a scheme to detect the presence of an eavesdropper (silent) and estimate its position. In general there are two reasons why we select transmitter side detection of the eavesdropper. Molecule communication channels are generally one directional and receivers cannot affect the transmission strategy easily. Furthermore, the rate of molecules absorbed at the receiver is generally quite small in value and cannot easily detect a distant eavesdropper's presence. For these two reasons, it is more practical to consider that the transmitter can determine to transmit secret information or not by itself based on the the received molecules at the transmitter side. At the transmitter ($x = 0$), it is clear that the presence of an eavesdropper will significantly reduce the number of returning molecules hitting it. If the molecules passing can be counted using a passive receiver without affecting the RW process, then the detection of the eavesdropper is possible. Passive receivers can be constructed using optical detectors, which can count and analyse molecules without capturing and consuming the molecules like chemical receivers do.

Let us assume that a transmitter ($x = 0$) with a passive detector, attempts to detect the molecules passing it after t seconds since a $\delta(t)$ pulse release. In the presence of a single primary receiver, the detected number is $\check{P}_1(0,L,t)$ - see Eq.(2). When a secondary eavesdropper is added, we showed that the resulting molecules detected is $\check{P}_{2a}(0,L,K,t)$ - see Eq.(5). Therefore, the difference is given by

$$\begin{aligned} \Delta P_{\mathrm{Tx}} &= \check{P}_1(x=0,L,t) - \check{P}_{2a}(x=0,L,K,t) \\ &= \sum_{n=-\infty,n\neq 0}^{+\infty} -P(-x_a,t) + \sum_{n=+2}^{+\infty} P(-x_b,t) + \sum_{n=-1}^{-\infty} P(-x_c,t), \end{aligned} \tag{9}$$

where x_a, x_b, and x_c are given below Eq. (5) and are all a function of the eavesdroppers's relative location K.

A. First Order Approximation

By examining Eq. (9), one can see that it is an infinite sum of negative exponential functions, which decay in value rapidly with increased distance from the emitter (increased $|n|$). In order to obtain a tractable location estimator, we only consider the dominant term (nearest mirror, i.e., $|n| = 1$), such that $\Delta P_{\mathrm{Tx}}(x = 0) \approx P(2K,t) - 2P(2(L+K))$. We note that within this, the $P(2K,t)$ term dominates, provided that L is sufficiently large. Therefore, the estimated eavesdropper's distance ($\tilde{K}_{\mathrm{Tx}}$) from the transmitter can be derived by solving for K in Eq. (9):

$$\tilde{K}_{\mathrm{Tx}} = \sqrt{-Dt\log((4\pi Dt)^{1/2}\Delta P_{\mathrm{Tx}})}, \tag{10}$$

where the time t can be interpreted as the expected propagation time for diffusion from transmitter to receiver. The approximate estimate of K is independent of the primary receiver's location L. The accuracy of this approximation is presented in terms of the distance estimation error ($\frac{|\tilde{K}_{\mathrm{Tx}}-K|}{K}$) below. That is to say, by detecting the shortfall in the number of molecules (ΔP_{Tx}), the first strongest term of Eq.(9) is sufficient to reverse estimate the distance of K. This reduces the complexity of numerically estimating K from the infinite series.

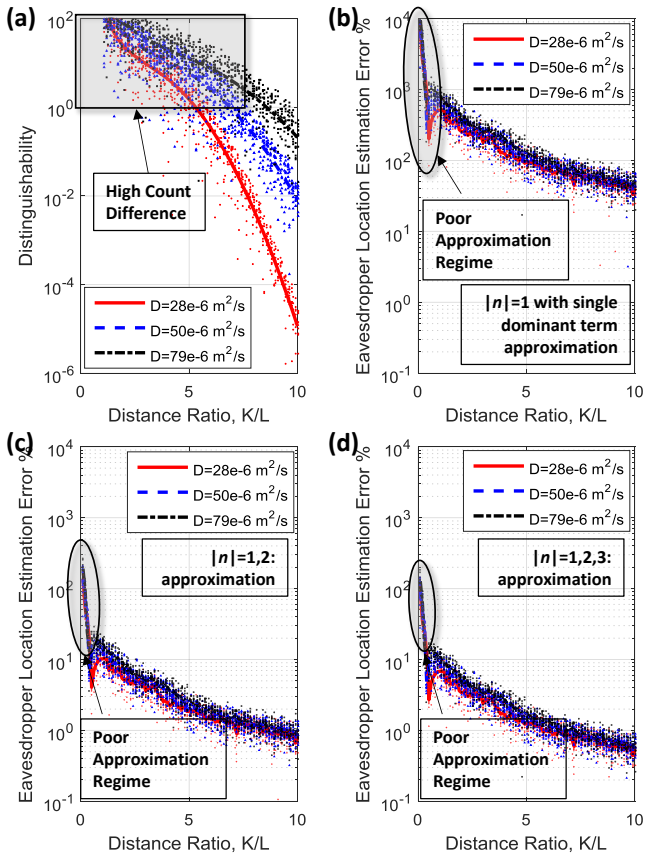

Fig. 4. Eavesdropper detection and localization results: (a) Distinguishability: ratio change in hitting probability $\Delta P_{\text{Tx}}/\tilde{P}_{2a}(0, L, t)$, and (b-d) Estimation error that results from first order $|n| = 1$ dominant term approximation, $|n| = 1, 2$ approximation, and $|n| = 1, 2, 3$ approximation. Parameters: $t = 0.1$s, and $L = 1$mm.

B. Differentiability and Accuracy Results

The results shown in Fig. 4**a** show that a higher diffusion coefficient and a closer eavesdropper location (small K/L) will increase the ratio change $\Delta P_{\text{Tx}}/\tilde{P}_{2a}(0, L, t)$, allowing for higher signal variation and easier distinguishability of the eavesdropper's existence from noise. This is intuitive, as an eavesdropper very close to the transmitter will absorb more molecules and its existence is easily detectable. The combined results in Fig. 4 show the following: a closer eavesdropper yields higher distinguishability (subplot a), but when the first order approximation and dominant term is applied for tractability reasons, a closer eavesdropper also causes higher error percentages (subplot b). Using exhaustive search, the location can be found for higher order approximations (subplot c-d), and the error is reduced significantly. Therefore, at low K/L ratios, low complexity numerical methods need to be used to estimate the eavesdropper's location (K) in the infinite series given in Eq.(9), which is the subject of future work. The rapid changes in error at low K values are purely a result of poor approximation accuracy due to only considering the first order.

In general, uncertainly in estimating the eavesdropper's location from sensing the discrepancies from molecule count is subject to counting noise from the stochastic arrival of molecules. It has been shown that the binomial distributed noise can be approximated to a Normal distribution [2]. We add the noise to the molecules counted by the sensor and the results in Fig. 4 show that the estimation error is quite sensitive to noise, but when using higher order approximations and for non-small K/L values, the error can be reduced to below 10%.

IV. Conclusions

In this paper, we demonstrated the potential of accurate passive eavesdropper detection and localization in molecular communications. Eavesdropper detection is made possible due to the fact that the random walk process has a finite return probability, and the existence of an absorbing eavesdropper acts as a detectable energy sink of which its location can be reverse estimated. The main contribution of the paper is the development of a detection scheme whereby the transmitter employs a passive receiver to count discrepancies in the number of molecules passing. Eavesdroppers that are stationed close to the transmitter can be easily identified, but complex numerical calculations are needed to reverse-estimate its location. For a eavesdropper that is further away from the transmitter than the primary receiver ($K > L$), the location can be estimated using a simple first term approximation and achieve a high accuracy, especially for low diffusion coefficient values. Future work will focus on expanding the framework to consider multiple eavesdroppers in higher dimensions, and expanding the applicability to the field of graph theory with sinks.

References

[1] I. Akyildiz, M. Pierobon, S. Balasubramaniam, and Y. Koucheryavy, "The internet of Bio-Nano things," *IEEE Communications Magazine*, vol. 53, no. 3, pp. 32–40, Mar. 2015.

[2] N. Farsad, H. B. Yilmaz, A. Eckford, C.-B. Chae, and W. Guo, "A comprehensive survey of recent advancements in molecular communication," *IEEE Communications Surveys and Tutorials*, 2016.

[3] L. Felicetti, M. Femminella, G. Reali, and P. Lio, "A molecular communication system in blood vessels for tumor detection," in *ACM Nanocom*, 2014.

[4] Y. Chahibi, M. Pierobon, S. O. Song, and I. F. Akyildiz, "A molecular communication system model for particulate drug delivery systems," *IEEE Transactions on Biomedical Engineering*, vol. 60, no. 12, pp. 3468–3483, 2013.

[5] V. Loscri, C. Marchal, N. Mitton, G. Fortino, and A. Vasilakos, "Security and Privacy in Molecular Communication and Networking: Opportunities and Challenges," *IEEE Transactions on Nanobioscience*, vol. 13, no. 3, 2014.

[6] F. Dressler and F. Kargl, "Towards security in nano-communication: Challenges and opportunities," *Nano Communication Networks*, vol. 3, no. 3, pp. 151–160, 2012.

[7] A. Mukherjee and A. Swindlehurst, "Detecting passive eavesdroppers in the MIMO wiretap channel," in *IEEE International Conference on Acoustics, Speech and Signal Processing (ICASSP)*, Mar. 2012.

[8] W. Guo, T. Asyhari, N. Farsad, H. Yilmaz, A. Eckford, and C. Chae, "Molecular communications: Channel model and physical layer techniques," *IEEE Wireless Communications*, Aug. 2016.

[9] Y. Kantor and M. Kardar, "Anomalous diffusion with absorbing boundary," *Physics Review E*, vol. 76, Dec. 2007.

[10] H. B. Yilmaz, A. C. Heren, T. Tugcu, and C.-B. Chae, "Three-Dimensional Channel Characteristics for Molecular Communications With an Absorbing Receiver," *IEEE Communications Letters*, vol. 18, no. 6, 2014.

[11] Y. Deng, A. Noel, M. Elkashlan, A. Nallanathan, and K. C. Cheung, "Molecular communication with a reversible adsorption receiver," in *IEEE International Conference on Communications (ICC)*, 2016.